Singular Trajectories in Airplane Cruise-Dash Optimization

Karl D. Bilimoria* and Eugene M. Cliff†
Virginia Polytechnic Institute and State University, Blacksburg, Virginia

The problem of determining optimal cruise-dash trajectories is examined for the case of time-fuel optimization using a linear combination of time and fuel as the performance index. These trajectories consist of a transient arc followed by a steady-state arc. For cases where the steady-state arc is flown at full throttle the associated skeletal transient trajectories are also flown at full throttle, and approach the cruise-dash points monotonically in an asymptotic fashion. When the steady-state arc is flown at an intermediate throttle setting, the transient trajectories follow a singular control law and exhibit a complex structure that is different from the full-throttle transients. Singular transients in the vicinity of singular cruise-dash points are confined to a bounded "singular surface." In state-space these trajectories trace out asymptotic spirals on the singular surface as they approach the steady-state arc. Addressing the question of optimality of the steady-state arc, it was found that although steady-state cruise fails a Jacobi-type condition, steady-state cruise-dash can satisfy this condition if the emphasis on time is sufficiently large. The outcome of the Jacobi-type test appears to be connected with the eigenstructure of the linearized state-adjoint system.

I. Introduction

THE problem of determining optimal flight trajectories for aircraft has been investigated by many researchers for a variety of performance indices. Time-optimal flight for a climb-dash mission has been investigated for the case of symmetric flight and is presented in Ref. 1. A nontrivial extension of this problem to a turn-climb-dash mission involving three-dimensional flight is reported in Ref. 2.

In contrast, fuel-optimal flight minimizes the fuel consumed while generally covering a specified range, and may require operation at an intermediate throttle setting. The optimality of steady-state cruise (operation at a fixed altitude and velocity pair) has been the subject of some debate.[3] Speyer[3] used the point-mass dynamic model and showed that for certain aeropropulsive models, steady-state cruise fails to satisfy a Jacobi-type condition obtained by a transformation to the frequency domain, and is therefore nonoptimal.

Between the two extremes of time-optimal and fuel-optimal flight (with range specified) is a spectrum of time-fuel-optimal flight conditions that may be regarded as members of a cruise-dash family. Such a situation arises when a linear combination of time and fuel is used as a performance index and can be regarded as an exercise in time-fuel tradeoff. Because of the time-scale separation found in aircraft dynamics,[4,5] the reduced-order cruise-dash model can be used to obtain the steady-state solution, and the full point-mass model can then be analyzed to obtain the transient solution. A first cut at the cruise-dash optimization problem was made[6] by considering the cruise-dash model that gives the steady-state or outer solution. In view of Speyer's findings[3] regarding the nonoptimality of steady-state cruise, this point is addressed in a later section where Speyer's analysis is retraced for steady-state operation at a cruise-dash point. This study focuses on transient trajectories that lead to steady-state operating points.

Received June 22, 1987; presented as Paper 87-2404 at the AIAA Guidance, Navigation and Control Conference, Monterey, CA, Aug. 17–19, 1987; revision received Oct. 29, 1987.

*Graduate Research Assistant, Aerospace and Ocean Engineering; currently Assistant Professor, Mechanical and Aerospace Engineering, Arizona State University, Tempe, AZ. Member AIAA.

†Professor, Aerospace and Ocean Engineering. Member AIAA.

II. Problem Formulation

Aircraft Equations of Motion in the Point-Mass Model

The equations of motion in the point-mass model may be written as

$$\dot{h} = V \sin\gamma \tag{1}$$

$$\dot{\gamma} = (g/V)(n - \cos\gamma) \tag{2}$$

$$\dot{V} = (g/W)[\eta T_{\max}(h,V) - D_o(h,V) - n^2 D_i(h,V)] - g \sin\gamma \tag{3}$$

$$\dot{x} = V \cos\gamma \tag{4}$$

$$\dot{W}_F = \eta Q_{\max}(h,V) \tag{5}$$

These equations are for symmetric flight in still air over a flat, nonrotating Earth. In these equations h is the altitude, V is the velocity (true airspeed), γ is the flight-path angle, x is the downrange, W_F is the weight of fuel consumed, g is the gravitational acceleration at sea level, and n is the load factor and is equal to the lift divided by the aircraft weight W. The maximum values of thrust and fuel flow rate are $T_{\max}$ and $Q_{\max}$, respectively. Both are represented as functions of altitude and velocity and are scaled by the throttle parameter η. This model embodies the assumptions of constant aircraft weight and thrust along the flight path (small angle of attack).

Optimal Control Problem

The problem under consideration is the determination of an atmospheric flight path that satisfies given initial and final conditions while minimizing a linear combination of time elapsed and fuel consumed. It is assumed that the range is sufficiently large to allow the decomposition of the trajectory into an initial transient, a steady state, and a terminal transient. In optimal control terms, this problem may be stated as: determine the controls n (load factor) and η (throttle setting) to transfer the dynamical system given by Eqs. (1–5) from a given set of initial states $(h_o,\gamma_o,V_o,x_o,W_{F_o})$ to a given set of final states (h_f,γ_f, V_f,x_f), while minimizing a Mayer-type cost function

$$\Phi = t_f + \mu W_F(t_f)$$

The parameter μ is specified as various values effecting a tradeoff between time and fuel. By varying the parameter μ, a family of cruise-dash trajectories is obtained with varying amounts of emphasis on time and fuel.[6]

The variational Hamiltonian[7,8] is formed by adjoining the right-hand sides of the system state differential Eqs. (1-5) with the costate variables (or Lagrange multipliers) $\lambda_h, \lambda_\gamma, \lambda_v, \lambda_x, \lambda_w$:

$$H = \lambda_h V \sin\gamma + \lambda_\gamma (g/V)(n - \cos\gamma) + \lambda_v [(g/W) \times (\eta T_{\max} - D_o - n^2 D_i) - g \sin\gamma] + \lambda_x V \cos\gamma + \lambda_w \eta Q_{\max} \tag{6}$$

The costate differential equations are

$$\dot{\lambda}_h = -\lambda_v (g/V)\eta T_{\max_h} - \lambda_w \eta Q_{\max_h} \tag{7}$$

$$\dot{\lambda}_\gamma = -\lambda_h V \cos\gamma - \lambda_\gamma (g/V) \sin\gamma + \lambda_v g \cos\gamma + \lambda_x \sin\gamma \tag{8}$$

$$\dot{\lambda}_v = -\lambda_h \sin\gamma + \lambda_\gamma (g/V^2)(n - \cos\gamma) - \lambda_v (g/W)(\eta T_{\max_v} - D_{o_v} - n^2 D_{i_v}) - \lambda_x \cos\gamma - \lambda_w \eta Q_{\max_v} \tag{9}$$

$$\dot{\lambda}_x = 0 \tag{10}$$

$$\dot{\lambda}_w = 0 \tag{11}$$

Equations (1-5) and (7-11) are the state-Euler equations. The problem of solving these equations with the appropriate boundary conditions is a two-point boundary-value problem (TPBVP). Generally, at the initial point, all five states are specified and the costates are free; whereas, at the final time, the fuel weight is free and the remaining four states are specified. Thus, at the final time all costates are free except for λ_w, which is specified to be equal to μ by the transversality condition.[7] At the final time, the transversality condition also requires that $H = -1$.

Using the Minimum Principle,[7,8] the control vector $\boldsymbol{u}$ may be determined from

$$\boldsymbol{u} = \arg[\min_{\boldsymbol{u}} H(\boldsymbol{u})] \tag{12a}$$

A necessary condition for unconstrained components of $\boldsymbol{u}$ that satisfy the Minimum Principle is

$$\frac{\partial H}{\partial \boldsymbol{u}} = 0 \tag{12b}$$

Substituting Eq. (6) in Eq. (12b) with the components of $\boldsymbol{u}$ as n and η yields

$$\frac{\partial H}{\partial n} = \lambda_\gamma \frac{g}{V} - \lambda_v 2n \frac{g}{W} D_i = 0 \tag{13}$$

$$\frac{\partial H}{\partial \eta} = \lambda_v \frac{g}{W} T_{\max} + \lambda_w Q_{\max} = 0 \tag{14}$$

Equation (13) can be solved to obtain the control n as

$$n = \frac{\lambda_\gamma}{\lambda_v} \left(\frac{W}{2D_i V} \right) \tag{15}$$

However, Eq. (14) does not yield the control η because it appears linearly in the expression for the Hamiltonian (6). In order to determine the control η, the switching function S is defined as

$$S = \lambda_v (g/W) T_{\max} + \lambda_w Q_{\max} \tag{16}$$

The control η must be chosen so as to minimize the Hamiltonian (6). Noting that η is bounded, the throttle control law derived from the Minimum Principle (12a) may be stated as

$$\text{If } S > 0, \text{ then } \eta = 0 \tag{17a}$$

$$\text{If } S < 0, \text{ then } \eta = 1 \tag{17b}$$

$$\text{If } S = 0 \text{ over a finite time interval, then } \eta = \eta_{\text{singular}} \tag{17c}$$

where $0 \le \eta_{\text{singular}} \le 1$.

Determination of Singular Control

The problem of determining a singular arc arises when application of the Minimum Principle in the form (12b) yields no information about the control, and the switching function is identically zero over a nonzero time interval. In such a case, the switching function S may be differentiated with respect to time until the singular control appears with a coefficient that is not identically zero.[9,10] If $(2k)$ time derivatives are required, then the *order* of the singular arc is (k). The singular control may then be obtained by solving the equation

$$\frac{d^{2k} S}{dt^{2k}} = 0$$

Along a singular arc one has

$$S = \lambda_v (g/W) T_{\max} + \lambda_w Q_{\max} = 0 \tag{18}$$

The thrust-specific fuel consumption (TSFC) is defined as the ratio

$$C(h,V) = [Q_{\max}(h,V)]/[T_{\max}(h,V)] \tag{19}$$

so that Eq. (18) may be written as

$$S = T_{\max}[\lambda_v (g/W) + \lambda_w C] = 0 \tag{20}$$

The time derivative of the switching function is

$$\dot{S} = T_{\max}[\dot{\lambda}_v (g/W) + \lambda_w \dot{C}] + \dot{T}_{\max}[\lambda_v (g/W) + \lambda_w C] \tag{21}$$

After some algebraic manipulation

$$(W/gT_{\max})\dot{S} = (1/V) + \lambda_\gamma (2g/V^2)(n - \cos\gamma) + \lambda_w \{[C_h (V/g) - C_v + (C/V)]W \sin\gamma + [(C/V) - C_v] \times (D_o + n^2 D_i) - C(D_{o_v} + n^2 D_{i_v})\} \tag{22}$$

It is convenient to define a function $G(h,\gamma,V,\lambda_\gamma,\lambda_w)$ as the right-hand side of Eq. (22). Note that the function G involves the load factor n, which can be expressed by a known function of the states and costates. From Eqs. (15) and (20)

$$n = -(\lambda_\gamma/\lambda_w)(g/2D_i CV) \tag{23}$$

Thus, along a singular arc, the load factor n is a function of h, V, λ_γ, and λ_w. We evaluate the derivatives n_h and n_v (for later use) as follows:

$$n_h = -n[(D_{i_h} C + D_i C_h)/D_i C] \tag{24}$$

$$n_v = -n[(D_{i_v} VC + D_i C + D_i VC_v)/D_i VC] \tag{25}$$

From Eq. (22)

$$\dot{S} = (g/W) T_{\max} G(h,\gamma,V,\lambda_\gamma,\lambda_w) \tag{26}$$

Therefore,

$$\ddot{S} = (g/W)T_{\max}\dot{G} + (g/W)\dot{T}_{\max}G \tag{27}$$

Using $\dot{S} = 0$ [Eq. (26)], we have

$$\ddot{S} = (g/W)T_{\max}\dot{G} \tag{28}$$

Hence,

$$(W/gT_{\max})\ddot{S} = (\dot{h}G_h + \dot{\gamma}G_\gamma + \dot{V}G_v + \dot{\lambda}_\gamma G_{\lambda_\gamma}) \tag{29}$$

where

$$\begin{aligned} G_h = {} & \lambda_\gamma[(2g/V^2)n_h] + \lambda_w\{[C_{hh}(V/g) - C_{vh} + (C_h/V)]W\sin\gamma \\ & - C_h(D_{o_v} + n^2D_{i_v}) + (D_{o_h} + n^2D_{i_h} + 2nn_hD_i)[(C/V) - C_v] \\ & + (D_o + n^2D_i)[(C_h/V) - C_{vh}] - C(D_{o_{vh}} + n^2D_{i_{vh}} + 2nn_hD_{i_v})\} \end{aligned} \tag{30}$$

$$\begin{aligned} G_v = {} & -(1/V^2) + \lambda_\gamma[(2g/V^2)n_v - (4g/V^3)(n - \cos\gamma)] \\ & + \lambda_w\{[C_{hv}(V/g) + (C_h/g) - C_{vv} + (C_v/V) - (C/V^2)]W\sin\gamma \\ & - C(D_{o_{vv}} + n^2D_{i_{vv}} + 2nn_vD_{i_v}) + [(C/V) - C_v] \\ & \times (D_{o_v} + n^2D_{i_v} + 2nn_vD_i) + [(C_v/V) - (C/V^2) - C_{vv}] \\ & \times (D_o + n^2D_i) - C_v(D_{o_v} + n_2D_{i_v})\} \end{aligned} \tag{31}$$

$$G_\gamma = \lambda_\gamma[(2g/V^2)\sin\gamma] + \lambda_w\{[C_h(V/g) - C_v + (C/V)]W\cos\gamma\} \tag{32}$$

$$\begin{aligned} G_{\lambda_\gamma} = {} & (2g/V^2)(2n - \cos\gamma) \\ & + (ng/D_iCV)\{CD_{i_v} + D_i[C_v - (C/V)]\} \end{aligned} \tag{33}$$

The switching function S has now been differentiated twice with respect to time and it can be seen from Eq. (29) that the singular control appears in the expression for S through the $\dot{V}$ term. Thus, the singular arc is of first order, unless the coefficient of η (which is $T_{\max}G_v$) is identically zero.

Setting $\ddot{S} = 0$

$$\eta = (D_o + n^2D_i)/T_{\max} + [W\sin\gamma/T_{\max} + \text{NUM/DEN}] \tag{34}$$

where

$$\text{NUM} = G_h\dot{h} + G_\gamma\dot{\gamma} + G_{\lambda_\gamma}\dot{\lambda}_\gamma \tag{35}$$

$$\text{DEN} = -(g/W)T_{\max}G_v \tag{36}$$

At equilibrium, the time derivatives of all states (except x and W_F) and costates are zero. Thus, it is clear that NUM in Eq. (35) will be equal to zero at equilibrium. The flight-path angle γ is also zero at equilibrium. As a result, the quantity in square brackets in Eq. (34) vanishes at equilibrium, and the steady-state control law is simply

$$\eta = (D_o + n^2D_i)/T_{\max} \tag{37}$$

evaluated at the cruise-dash point h^*, V^*. This is equivalent to stating that the thrust must equal drag, which is precisely what level-flight equilibrium requires. Thus, it can be seen that the singular control is made up of two distinct parts, one of which vanishes as the system approaches equilibrium.

III. Necessary Conditions

Generalized Legendre-Clebsch Condition

Since the throttle control appears linearly in the Hamiltonian (6), the Classical Legendre-Clebsch condition[7,8] is satisfied only in the weak form (i.e., as an equality). For such cases, the Generalized Legendre-Clebsch condition must be satisfied along a candidate extremal. The mathematical treatment for extending the Classical Legendre-Clebsch condition to cases where one or more of the controls is singular is given in Refs. 11 and 12. It is required that the matrix $[R]$ given below be positive-semidefinite.

$$[R]_{(m\times m)} = \begin{bmatrix} R_1 & R_2^T \\ R_2 & R_3 \end{bmatrix} \geq 0 \tag{38}$$

For the problem under consideration $m = 2$, and the submatrices R_1, R_2, and R_3 are scalars. Positive semidefiniteness of the matrix $[R]$ requires that all of the following three conditions hold:[13]

$$R_1 = \frac{\partial^2 H}{\partial n^2} \geq 0 \tag{39a}$$

$$R_3 = -\frac{\partial}{\partial\eta}\left[\frac{\mathrm{d}^2}{\mathrm{d}t^2}\left(\frac{\partial H}{\partial\eta}\right)\right] \geq 0 \tag{39b}$$

$$(R_1R_3 - R_2^2) \geq 0 \tag{39c}$$

where

$$R_2 = \frac{\partial}{\partial\eta}\left[\frac{\mathrm{d}}{\mathrm{d}t}\left(\frac{\partial H}{\partial n}\right)\right]$$

The first condition (39a) is the Classical Legendre-Clebsch Condition applied to the nonsingular (quadratic) control n, the second condition (39b) is the Kelley Condition applied to the singular (linear) control η, and the third condition (39c) is the Goh Condition that involves both singular and nonsingular controls.

Erdmann Corner Condition

The state and costate variables in the state-Euler equations are continuous and have continuous first time-derivatives for cases where the control variables are continuous. However, if any control variable *jumps* (is discontinuous), then the first time-derivatives of the states will, in general, be discontinuous. If this is the case we have a *broken extremal*[14] or a *corner*. At a corner (or junction of two extremals) the Erdmann Corner Condition[14,15] must be satisfied. This condition requires that all the costate variables be continuous at a corner.

McDanell-Powers Junction Condition

The joining of singular and nonsingular arcs generally involves a jump in the singular control variables and, hence, the junction is a corner. Therefore, the Erdmann Corner Condition applies at the junction of singular and nonsingular arcs. Additionally, the McDanell-Powers Junction Condition[16] applies: if r is the lowest-order derivative of the (singular) control that is discontinuous at the junction, and if q is the order of the singular arc, then $(q + r)$ must be an odd integer.

For a first-order singular arc ($q = 1$), this condition may be interpreted as follows:

1) If the singular control is unsaturated at a junction, then it can jump to either the upper or lower bound ($r = 0$).

2) If the singular control saturates at a junction with a nonzero time derivative, it *must* jump to the opposite bound ($r = 0$).

3) If the singular control saturates at a junction with a zero time derivative, it can either jump to the opposite bound ($r = 0$) or stay at the same bound ($r = 2$).

IV. Numerical Results and Discussion

Application of the Minimum Principle to the flight-path optimization problem at hand results in a nonlinear TPBVP where some of the boundary conditions are known at one

boundary and the rest at the other boundary. A multiple shooting package was used along with data for a high-performance interceptor aircraft in a computational study of cruise-dash trajectories.

General Structure of Cruise-Dash Trajectories

As discussed in Sec. II, an optimal trajectory for the cruise-dash problem is a composite consisting of a transient part and a steady-state part. Steady-state cruise-dash has been studied in an earlier work,[6] and optimal steady-state operating points have been computed over the entire spectrum of interest from the dash point through the cruise point to the endurance point. These are shown in Fig. 1 along with the military and afterburning flight envelopes.

In general, the initial operating conditions will not coincide with the appropriate steady-state conditions, and the aircraft must fly a transient trajectory that leads to the cruise-dash operating point. Along this part of the trajectory the altitude, velocity, and path angle as well as the controls n and η will in general be time-varying.

Full-Throttle Cruise-Dash Trajectories

For cruise-dash trajectories associated with small values of μ (i.e., light emphasis on fuel), it can be seen from Fig. 1 that the associated cruise-dash points lie on the flight envelope and correspond to full-throttle operation. It is reasonable to conjecture that the transients leading to these points will also be run at full throttle.

Full-throttle trajectories were computed for all values of μ that yield *steady-state operating points* where $\eta = \eta_{\max}$. It was found that for all computed trajectories the switching function remained negative for all times, confirming that the computed full-throttle trajectories satisfy the Minimum Principle. These trajectories correspond to a certain range of low values of the time-fuel tradeoff parameter μ (0.0 s/lb to 0.1328 s/lb) indicating a heavy emphasis on time. Each of these transient trajectories leads to a steady-state operating point that lies on the afterburning flight envelope. Figure 2 shows several full-throttle cruise-dash trajectories for values of μ ranging from 0.0 s/lb to 0.1328 s/lb in the (h,V) plane along with a portion of the afterburning flight envelope.

Partial-Throttle Cruise-Dash Trajectories

It can be seen from Fig. 1 that beyond a certain value of μ the steady-state operating points lie inside the flight envelope, indicating that the throttle control is not at its bound along the steady-state cruise-dash arc. The steady-state cruise-dash arc is, in fact, a singular arc featuring a singular throttle control lying between its bounds. Correspondingly, the switching function and its time derivative are zero along this arc. It is conjectured that if the steady-state cruise-dash arc involves a singular control, then the transient arc leading to the steady state also exhibits the same feature, at least in the vicinity of the cruise-dash arc.

Singular Surface

The transient dynamics of the (sixth-order) system defined by the state-Euler equations involve the three "nonignorable" states h, V, and γ and their associated costates λ_h, λ_v, and λ_γ.

It was determined from an eigenvalue analysis that two modes of the linearized system (corresponding to purely real eigenvalues) violate the conditions $S = 0$ and $\dot{S} = 0$, which all singular arcs must satisfy. Therefore, all singular arcs in the linearized system must be confined to a four-dimensional linear subspace where the two "nonsingular" modes are inactive. For the linearized system this is a four-dimensional plane, corresponding to a four-dimensional *singular manifold* in the actual nonlinear system. Out of the four modes, only two will be stable due to the structure of the associated eigenvalues. Hence, all singular trajectories *that lead to the equilibrium point* in the

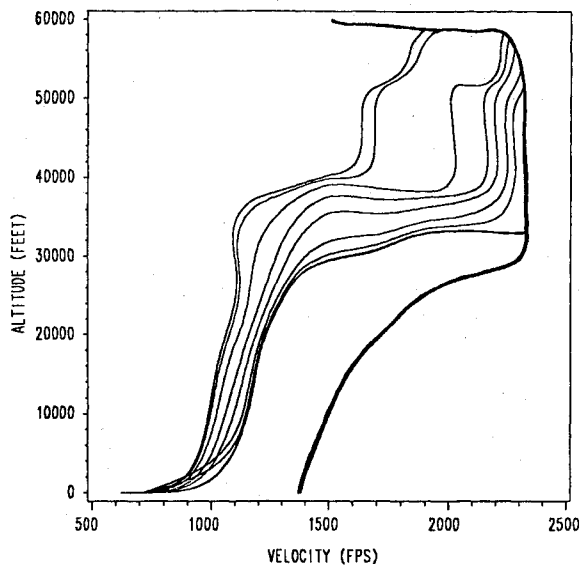

Fig. 2 Full-throttle cruise-dash trajectories.

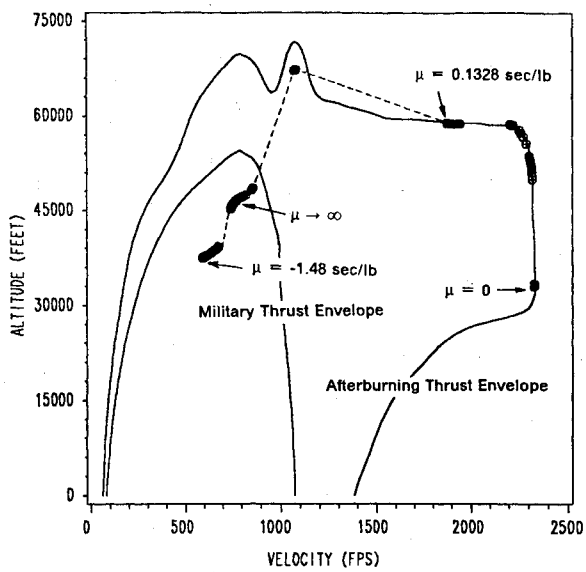

Fig. 1 Cruise-dash points in (h,V) plane.

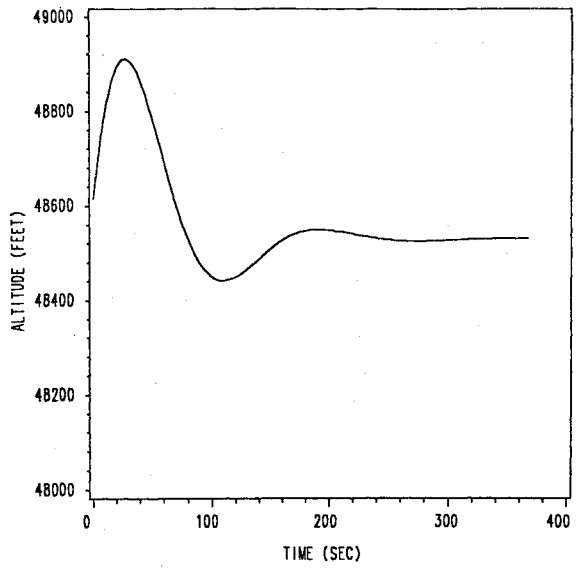

Fig. 3 Altitude time history for singular trajectory.

linearized system must lie in a two-dimensional linear subspace (i.e., on a plane). Thus, in the actual nonlinear system the singular manifold may be regarded as a *singular surface* in (h,V,γ) space.

Singular Trajectories to the Equilibrium Point

A singular trajectory was computed by making a small perturbation about the equilibrium point and then integrating the state-Euler equations backwards in time. The perturbation in the states and costates was proportional to the eigenvectors that correspond to the complex eigenvalues of the linearized system. Four such combinations were used to create a perturbation, and the corresponding singular trajectories were generated by backward integration of the state-Euler equations that define the actual nonlinear system with $\mu = 320$ s/lb (heavy emphasis on fuel). The integration was performed with monitoring of the value of the singular control and the values of the switching function and its time derivative, and was stopped when the control saturated at its upper bound. The switching function and its time derivative remained zero all along the trajectory. The altitude and control throttle histories of one such trajectory are shown in Figs. 3 and 4. It was found that all three (nonignorable) states undergo damped oscillations that die out as the equilibrium point is approached, as predicted by the linearized model. Figure 5 shows all four trajectories in (h,V,γ) space. These trajectories approach the equilibrium point along asymptotic spirals, which define the singular surface in (h,V,γ) space.

Composite Bang-Singular Trajectories

If the initial operating point happens to lie on the singular surface, then the transient trajectory is purely singular and describes an asymptotic spiral in (h,V,γ) space fairing into the equilibrium point. However, if the initial states do not correspond to a point the lies on the singular surface, the transient trajectory would have a more complex structure. In general, it would consist of two segments: an initial nonsingular arc run at either full throttle or zero throttle (or possibly a combination thereof) until the singular surface is reached, followed by a purely singular arc that takes the system to the equilibrium point. Thus, the singular surface may be regarded as a "switching surface" in state-space. The joining of a singular and a nonsingular arc is subject to the McDanell-Powers Junction Condition discussed in Sec. III. According to these conditions, if the singular control is unsaturated at a junction, then it can jump to either its upper or lower bound. Two such trajectories were computed, and their throttle control histories are shown in Figs. 6 and 7.

Necessary Conditions

All the trajectories computed and discussed in this section were found to satisfy all the necessary conditions outlined in Sec. III. The singular trajectories satisfy the Generalized Legendre-Clebsch Condition along their entire length, as do the singular segments of composite bang-singular trajectories. The junctions of the composite bang-singular trajectories are in accordance with the McDanell-Powers Junction Condition, and the Erdmann Corner Condition is also satisfied (the costates are continuous). No Jacobi-type condition was checked along the transient singular arc.

V. Jacobi-type Condition

In the foregoing discussion, it has been stated that the structure of candidate extremals is a transient arc followed by a

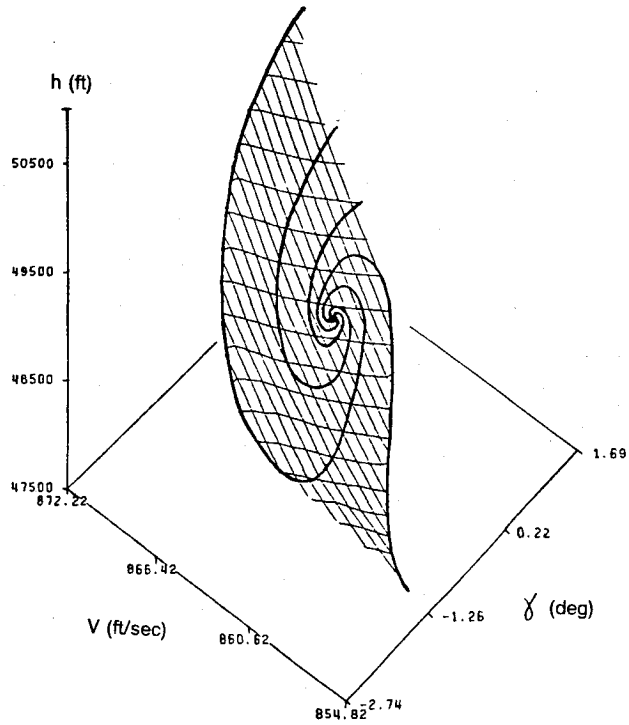

Fig. 5 Singular surface and trajectories in (γ,h,V) space.

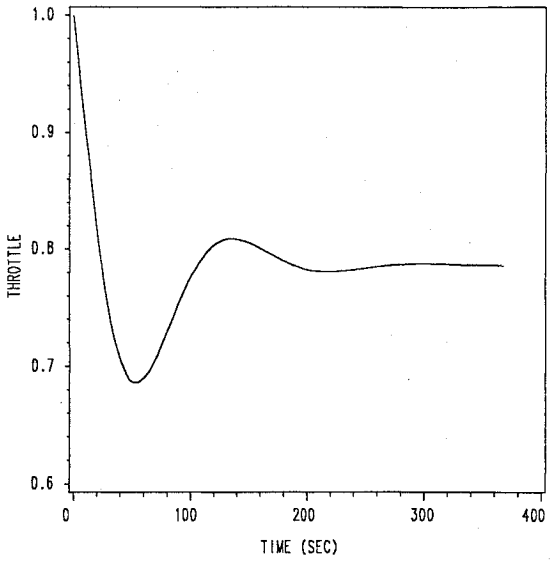

Fig. 4 Throttle time history for singular trajectory.

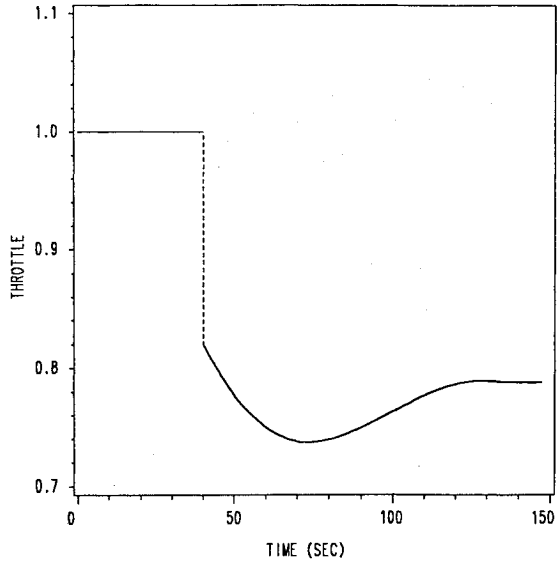

Fig. 6 Bang-singular throttle control (case 1).

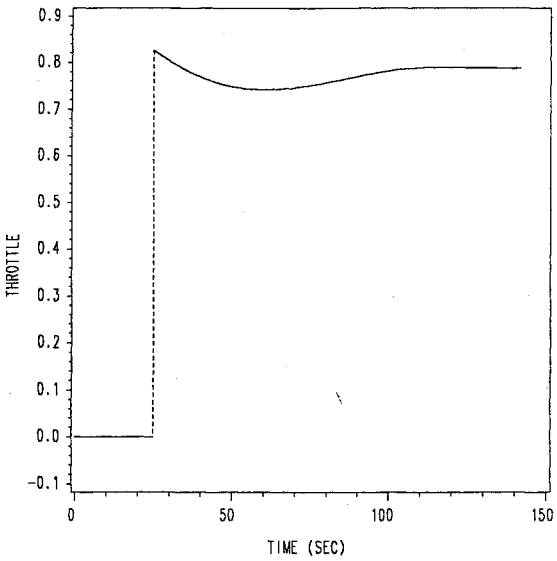

Fig. 7 Bang-singular throttle control (case 2).

steady-state cruise-dash arc. For a performance index involving fuel alone, Speyer[3] cast doubt on the optimality of a steady-state *cruise* arc by showing that for certain aeropropulsive models a Jacobi-type condition is not satisfied. The Jacobi condition in the calculus of variations[14,15] is not applicable when some or all components of the controls are singular. In such cases, the accessory minimum problem (AMP) is formulated and the Goh transform is applied. The transformed AMP is nonsingular and the classical Jacobi condition may now be applied in one of several forms.[17] The approach taken by Speyer is to use Parseval's transformation and then apply the Jacobi test in the frequency domain. For a specialized drag model, Eq. (62) of Ref. 3 states this Jacobi-type condition as follows:

$$Y(\omega) = H_{LL} - \{\sigma/[m^2V^2D_{vv}(\omega^2-\beta g)^2]\}[\omega^2(W^2/V^2) + V^2D_{vh}^2] \tag{40}$$

must be nonnegative for all values of ω. Although H_{LL} is positive, it is seen that $Y(\omega)$ can be made negative for values of ω near $\sqrt{\beta g}$. Note that the cost function to be minimized in this problem is fuel alone. Retracing Speyer's analysis for the exact model, with a linear combination of time and fuel as the performance index, one gets

$$Y(\omega) = H_{LL} - \{\sigma/[m^2V^2D_{vv}(\omega^2 - \beta g)^2]\} \times [\omega^2(W^2/V^2) + V^2D_{vh}^2 - \omega^2(\nu VD_{vv}/\sigma)] \tag{41}$$

where ν is a time-fuel tradeoff parameter that can be expressed as a function of μ. It can be shown that $Y(\omega)$ will be nonnegative for all values of ω if

$$\nu \geq \frac{\sigma}{D_{vv}}[(VD_{vh}^2/\beta g) + (W^2/V^3)] \tag{42}$$

For the case of $\nu = 0$ ($\mu \to \infty$), there is no emphasis on time, and Speyer's result is recovered. However, if there is a sufficiently heavy emphasis on time and ν is large enough (μ is small enough) then Eq. (42) will be satisfied. As a consequence, Speyer's Jacobi-type condition will be satisfied for steady-state cruise-dash arcs corresponding to a sufficiently heavy emphasis on time. Thus, for the model studied by Speyer, it has been shown that although steady-state *cruise* fails a Jacobi-type test and is nonminimizing, some types of steady-state *cruise-dash* pass this test and can be minimizing.

For the case of steady-state cruise-dash, a Jacobi-type test may be applied[17] by examining solutions of the algebraic matrix Ricatti equation.[18] The Jacobi-type condition is satisfied if the solution matrix to the algebraic matrix Ricatti equation is finite, real, and positive semidefinite. Using the aeropropulsive data for the example aircraft, this matrix was evaluated numerically for several steady-state cruise-dash conditions corresponding to various values of μ. It was found that for large values of μ (conditions approximating cruise), the Jacobi-type condition was not satisfied since the solution matrix to the algebraic matrix Ricatti equation had complex entries. If a substantial emphasis was placed on time (moderate values of μ) then the Jacobi-type condition was satisfied. An interesting feature that emerged from this study was that the Jacobi-type condition was satisfied when the eigenvalues of the linearized system had no purely imaginary values, and failed the test when this structure collapsed.

VI. Conclusions

It has been established computationally that skeletal cruise-dash trajectories associated with a light emphasis on fuel (and heavy emphasis on time) are run at full throttle. The steady-state operating points lie on the flight envelope, and the skeletal transients leading to those optimal operating points are flown with the throttle at its maximum limit. These transients approach the steady-state cruise-dash points in an asymptotic fashion. Moreover, the state histories in the vicinity of the equilibrium points are monotonic with no oscillations.

Cruise-dash trajectories corresponding to a heavy emphasis on fuel (and light emphasis on time) have a different and far more complex structure. The steady-state operating points lie within the flight envelope, and the corresponding steady-state cruise-dash arc is a singular arc flown with a partial-throttle setting. Studies of the transient trajectories leading to some of these cruise-dash points reveal that they approach the steady-state asymptotically in a damped oscillatory fashion, unlike the full-throttle trajectories studied earlier. These transient trajectories in the neighborhood of the equilibrium points are singular trajectories, and are run with partial-throttle settings. A singular control law has been derived for the throttle settings.

Transient singular trajectories in the neighborhood of the equilibrium point lie on a two-dimensional singular surface in the three-dimensional (h,V,γ) state-space. On this surface, transient singular trajectories fair into the equilibrium (cruise-dash) point along asymptotic spirals. The singular surface appears to be bounded as a result of saturation of the throttle control at its upper limit. If the initial states lie outside the singular surface, a full-throttle or zero-throttle trajectory must be flown to the singular surface, after which a singular trajectory takes the system to the steady state.

It has been determined that, for the example aircraft, steady-state operation at a cruise-dash point does satisfy the Jacobi-type condition for certain values of μ and, therefore, steady-state cruise-dash can be optimal. However, steady-state cruise-dash arcs fail a Jacobi-type test for large values of μ, and in particular the cruise arc fails the Jacobi-type test. The Jacobi-type test has a strong connection with the eigenstructure of the linearized system at the equilibrium point. Specifically, if the eigenvalues have no purely imaginary values, the Jacobi-type condition is satisfied. Absence of this feature (presence of purely imaginary eigenvalues) results in failure of the Jacobi-type condition.

Acknowledgments

This research was supported in part by DARPA under ACMP Contract F49620-87-C-0116 and by NASA Langley Research Center under Grant NAG 1-203. Dr. Christopher Gracey served as NASA Technical Officer. The authors would like to thank Professor Henry J. Kelley for valuable discussions during the course of this work.

References

[1]Weston, A. R., Kelley, H. J., and Cliff, E. M., "Onboard Near-Optimal Climb-Dash Energy Management," *Journal of Guidance, Control, and Dynamics*, Vol. 8, May-June 1985, pp. 320–324.

[2]Visser, H. G., Kelley, H. J., and Cliff, E. M., "Energy Management of Three-Dimensional Minimum-Time Intercept," *Journal of Guidance, Control, and Dynamics*, Vol. 10, Nov.-Dec. 1987, pp. 574–580.

[3]Speyer, J. L., "Nonoptimality of the Steady-State Cruise for Aircraft," *AIAA Journal*, Vol. 14, Nov. 1976, pp. 1604–1610.

[4]Ardema, M. D. and Rajan, N., "Separation of Time Scales in Aircraft Trajectory Optimization," *Journal of Guidance, Control, and Dynamics*, Vol. 8, March-April 1985, pp. 275–278.

[5]Kelley, H. J., "Reduced-Order Modeling in Aircraft Mission Analysis," *AIAA Journal*, Vol. 9, Feb. 1971, pp. 349–350.

[6]Bilimoria, K. D., Cliff, E. M., and Kelley, H. J., "Classical and Neo-Classical Cruise-Dash Optimization," *Journal of Aircraft*, Vol. 22, July 1985, pp. 555–560.

[7]Bryson, A. E. and Ho, Y. C., *Applied Optimal Control*, Hemisphere, Washington, DC, 1969.

[8]Leitmann, G., *An Introduction to Optimal Control*, McGraw-Hill, New York, 1966.

[9]Bell, D. J. and Jacobson, D. H., *Singular Optimal Control Problems*, Academic, New York, 1975.

[10]Kelley, H. J., Kopp, R. E., and Moyer, H. G., "Singular Extremals," *Topics in Optimization*, edited by G. Leitmann, Academic, New York, 1967.

[11]Goh, B. S., "The Second Variation for the Singular Bolza Problem," *SIAM Journal on Control*, Vol. 4, No. 2, May 1966, pp. 309–325.

[12]Goh, B. S., "Necessary Conditions for Singular Extremals Involving Multiple Control Variables," *SIAM Journal on Control*, Vol. 4, No. 4, Nov. 1966, pp. 717–731.

[13]Prussing, J. E., "The Principal Minor Test for Semidefinite Matrices," *Journal of Guidance, Control, and Dynamics*, Vol. 9, Jan.-Feb. 1986, pp. 121–122.

[14]Gelfand, I. M. and Fomin, S. V., *Calculus of Variations*, Prentice-Hall, New York, 1963.

[15]Ewing, G. M., *Calculus of Variations with Applications*, Dover, New York, 1985.

[16]McDanell, J. P. and Powers, W. F., "Necessary Conditions for Joining Singular and Nonsingular Subarcs," *SIAM Journal on Control*, Vol. 9, No. 2, May 1971, pp. 161–173.

[17]McDanell, J. P. and Powers, W. F., "New Jacobi-Type Necessary and Sufficient Conditions for Singular Optimization Problems," *AIAA Journal*, Vol. 8, Aug. 1970, pp. 1416–1420.

[18]Kwakernaak, H. and Sivan, R., *Linear Optimal Control Systems*, Wiley Interscience, New York, 1972.